



# Identification and Integrate Analysis of Key Biomarkers for Diagnosis and Prognosis of Non-Small Cell Lung Cancer Based on Bioinformatics Analysis

Technology in Cancer Research & Treatment  
 Volume 20: 1-15  
 © The Author(s) 2021  
 Article reuse guidelines:  
[sagepub.com/journals-permissions](https://sagepub.com/journals-permissions)  
 DOI: 10.1177/15330338211060202  
[journals.sagepub.com/home/tct](https://journals.sagepub.com/home/tct)  


Ke Gong, MBBS<sup>1,\*</sup>, Huiling Zhou, MBBS<sup>1,\*</sup>, Haidan Liu, Ph.D<sup>2</sup>,  
 Ting Xie, Ph.D<sup>1</sup>, Yong Luo, MBBS<sup>1</sup>, Hui Guo, MBBS<sup>1</sup>, Jinlan Chen, Ph.D<sup>1</sup>,  
 Zhiping Tan, Ph.D<sup>2</sup>, Yifeng Yang, Ph.D<sup>1</sup>, and Li Xie, Ph.D<sup>1</sup> 

## Abstract

**Background:** Non-small cell lung cancer (NSCLC) is the most common type of lung cancer affecting humans. However, appropriate biomarkers for diagnosis and prognosis have not yet been established. Here, we evaluated the gene expression profiles of patients with NSCLC to identify novel biomarkers. **Methods:** Three datasets were downloaded from the Gene Expression Omnibus (GEO) database, and differentially expressed genes were analyzed. Venn diagram software was applied to screen differentially expressed genes, and gene ontology functional analysis and Kyoto Encyclopedia of Genes and Genomes (KEGG) pathway analysis were performed. Cytoscape was used to analyze protein-protein interactions (PPI) and Kaplan–Meier Plotter was used to evaluate the survival rates. Oncomine database, Gene Expression Profiling Interactive Analysis (GEPIA), and The Human Protein Atlas (THPA) were used to analyze protein expression. Quantitative real-time polymerase (qPCR) chain reaction was used to verify gene expression. **Results:** We identified 595 differentially expressed genes shared by the three datasets. The PPI network of these differentially expressed genes had 202 nodes and 743 edges. Survival analysis identified 10 hub genes with the highest connectivity, 9 of which (*CDC20*, *CCNB2*, *BUB1*, *CCNB1*, *CCNA2*, *KIF11*, *TOP2A*, *NDC80*, and *ASPM*) were related to poor overall survival in patients with NSCLC. In cell experiments, *CCNB1*, *CCNB2*, *CCNA2*, and *TOP2A* expression levels were upregulated, and among different types of NSCLC, these four genes showed highest expression in large cell lung cancer. The highest prognostic value was detected for patients who had successfully undergone surgery and for those who had not received chemotherapy. Notably, *CCNB1* and *CCNA2* showed good prognostic value for patients who had not received radiotherapy. **Conclusion:** *CCNB1*, *CCNB2*, *CCNA2*, and *TOP2A* expression levels were upregulated in patients with NSCLC. These genes may be meaningful diagnostic biomarkers and could facilitate the development of targeted therapies.

## Keywords

non-small cell lung cancer, gene expression omnibus database, bioinformatics analysis, prognosis, diagnosis, biomarkers

## Abbreviations

BiNGO, Biological Networks Gene Oncology Tool; BP, biological process; CC, cellular component; CI, confidence interval; DAVID, The Database for Annotation, Visualization, and Integrated Discovery; dDEG, downregulated differentially expressed gene; DEG, differentially expressed gene; FBS, fetal bovine serum; GO, Gene Ontology; GEO, Gene Expression Omnibus; GEPIA, Gene Expression Profiling Interactive Analysis; HR, hazard ratio; LUAD, lung adenocarcinoma; LUSC, lung squamous cell carcinoma; MF, molecular function; MCODE, Molecular Complex Detection; NSCLC, non-small cell lung cancer; PPI, protein-protein interaction; qPCR, quantitative real-time polymerase chain reaction; TCGA, The Cancer Genome Atlas; THPA, The Human Protein Atlas; uDEG, upregulated differentially expressed gene.

Received: May 20, 2021; Revised: September 25, 2021; Accepted: October 26, 2021.

<sup>1</sup> Department of Cardiovascular Surgery, The Second Xiangya Hospital of Central South University, Central South University, Changsha, PR China

<sup>2</sup> The Clinical Center for Gene Diagnosis and Therapy of The State Key Laboratory of Medical Genetics, The Second Xiangya Hospital of Central South University, Central South University, Changsha, Hunan, PR China

\*These authors contributed equally to this work and should be considered co-first authors

## Corresponding Author:

Li Xie, Department of Cardiovascular Surgery, The Second Xiangya Hospital of Central South University, Central South University, Changsha 410011, PR China.  
 xiel55@csu.edu.cn



Creative Commons Non Commercial CC BY-NC: This article is distributed under the terms of the Creative Commons Attribution-NonCommercial 4.0 License (<https://creativecommons.org/licenses/by-nc/4.0/>) which permits non-commercial use, reproduction and distribution of the work without further permission provided the original work is attributed as specified on the SAGE and Open Access page (<https://us.sagepub.com/en-us/nam/open-access-at-sage>).

## Introduction

Lung cancer is highly invasive and metastatic and is a major cause of cancer-related deaths. Non-small cell lung cancer (NSCLC), the most common of lung cancer, accounts for 85% of all lung cancers.<sup>1</sup> Despite major advances in the diagnosis and treatment of NSCLC with the development of medical technology in recent years, the 5-year survival rate of patients with NSCLC is only 17%.<sup>2</sup> Changes in social lifestyles and environments have led to an increase in the incidence of NSCLC, and approximately 234 000 new cases of NSCLC are reported in the United States of America each year.<sup>3,4</sup> Regardless of which therapeutic option is chosen, chemotherapy is still an essential adjuvant treatment for patients with lung cancer. However, serious adverse reactions can occur following administration of chemotherapy drugs, and the efficacy of these therapies is often not satisfactory.<sup>5,6</sup> Therefore, there is an urgent need for new treatment strategies to complement traditional chemotherapy. Moreover, with commencement of the genomic era and advancements in molecular biology research, molecular mechanisms of life phenomena and disease have attracted much attention, and recent research on NSCLC has focused on the identification of novel targets to facilitate the development of new molecular targeted drugs.

With the development of sequencing technology and large-scale sequencing research, large amounts of sequencing data have been collected in many databases.<sup>7</sup> To discover biomarkers and potential targets related to cancer, researchers can resequence the tumor and then re-analyze the tumor from gene to protein expression.<sup>8,9</sup> Furthermore, to avoid inaccurate experimental results owing to the use of multiple platforms or small sample sizes, comprehensive bioinformatics methods can be used to obtain valuable biological information in cancer research.<sup>10,11</sup>

Many novel targets and biomarkers of NSCLC have been reported in recent studies, providing substantial contributions to NSCLC research. For example, in a study by Hu et al. *miR-210* was found to serve as a potential biomarker for NSCLC detection, and they found that the use of a set of multiple biomarkers may be a more comprehensive indicator than the analysis of *miR-210* alone.<sup>12</sup> Additionally, Wang provided a dataset of NSCLC biomarkers with potential applications in prognosis and found that *TOP2A* may be a valuable biomarker for survival and prognosis in patients with NSCLC.<sup>13</sup> Saigusa and colleagues also revealed that new metabolites related to *NRF2* activity may be diagnostic biomarkers for *NRF2* activation, providing important insights into the selective toxicity of new metabolic nodes in *NRF2*-activated NSCLC.<sup>14</sup> Despite these findings, NSCLC remains a complex and diverse disease, and more genetic data and biological information are needed to improve diagnosis and treatment strategies.

In the present study, we selected three datasets, ie, GSE18842,<sup>15</sup> GSE44077,<sup>16</sup> and GSE19804,<sup>17</sup> from the Gene Expression Omnibus (GEO) database and conducted various bioinformatics analyses to evaluate gene expression and protein interactions in NSCLC tumor tissues, with the aim of

elucidating the underlying molecular mechanisms in NSCLC and for establishing novel biomarkers for its diagnosis and treatment.

## Materials and Methods

The gene expression profile data (GSE18842, GSE44077, and GSE19804) were downloaded from GEO (Supplementary Tables S1-S3).<sup>18</sup> The inclusion criteria for gene expression data were as follows: (1) the samples used for analysis were tissues, (2) all tissues were categorized as NSCLC or normal tissues, (3) samples were collected from the same species group, (4) probes could be converted, (5) complete information was available for analysis, and (6) the sample size of each study was larger than 10 samples. The array data for GSE18842 included 46 NSCLC tumor and 45 normal tissues as the control group. GSE19804 included 60 NSCLC tumors and 60 adjacent normal tissues. GSE44077 was composed of 66 tumor tissues and 55 normal tissues.

GEO2R was used to analyze differentially expressed genes (DEGs) between NSCLC samples and normal samples (<http://www.ncbi.nlm.nih.gov/geo/geo2r>). GEO2R is a web tool that can be used to compare and analyze DEGs in NSCLC samples and normal lung tissue samples through the Limma and GEOquery R packages of the Bioconductor project. Adjusted *P* values and  $|\log_2$  fold change| ( $|\log_2FC|$ ) values were used to assess the significance of DEGs, and the cut-off criteria were set as  $|\log_2FC| > 1$  and adjusted *P* value  $< .01$ .

Venn diagram software in the Bioinformatics & Evolutionary Genomics platform (<http://bioinformatics.psb.ugent.be/webtools/Venn/>) was used to perform intersection analysis on the DEGs of our three independent samples. We screened out genes that were differentially expressed in the three independent samples and determined whether the selected genes were up- or downregulated based on  $\log_2FC$  values of DEGs between NSCLC and normal tissues.

Gene Ontology (GO), a commonly used bioinformatics tool for comprehensive evaluation of gene function; Kyoto Encyclopedia of Genes and Genomes (KEGG), a database for annotation of the advanced functions of biological systems at the molecular level; and the Database for Annotation, Visualization, and Integrated Discovery (DAVID; <https://david.ncifcrf.gov/>), an online tool for enriching and analyzing bioinformatics resources.<sup>19</sup> were used to clarify gene functions and functional enrichment. Upregulated DEGs (uDEGs) and downregulated DEGs (dDEGs) were identified using DAVID for the three gene expression profile datasets. The cut-off criterion was set as a *P* value less than 0.05.

The STRING (<http://string-db.org/>) database, a search tool for retrieving interacting genes and providing important information regarding protein-protein interactions (PPIs),<sup>20</sup> was used to construct a PPI network of DEGs, and Cytoscape (version 3.7.2) was used to process and analyze the PPI network.<sup>21</sup> The cut-off criterion was a combined score greater than or equal to 0.9. Subsequently, we used a Cytoscape plug-in Molecular Complex Detection (MCODE) to detect important modules in

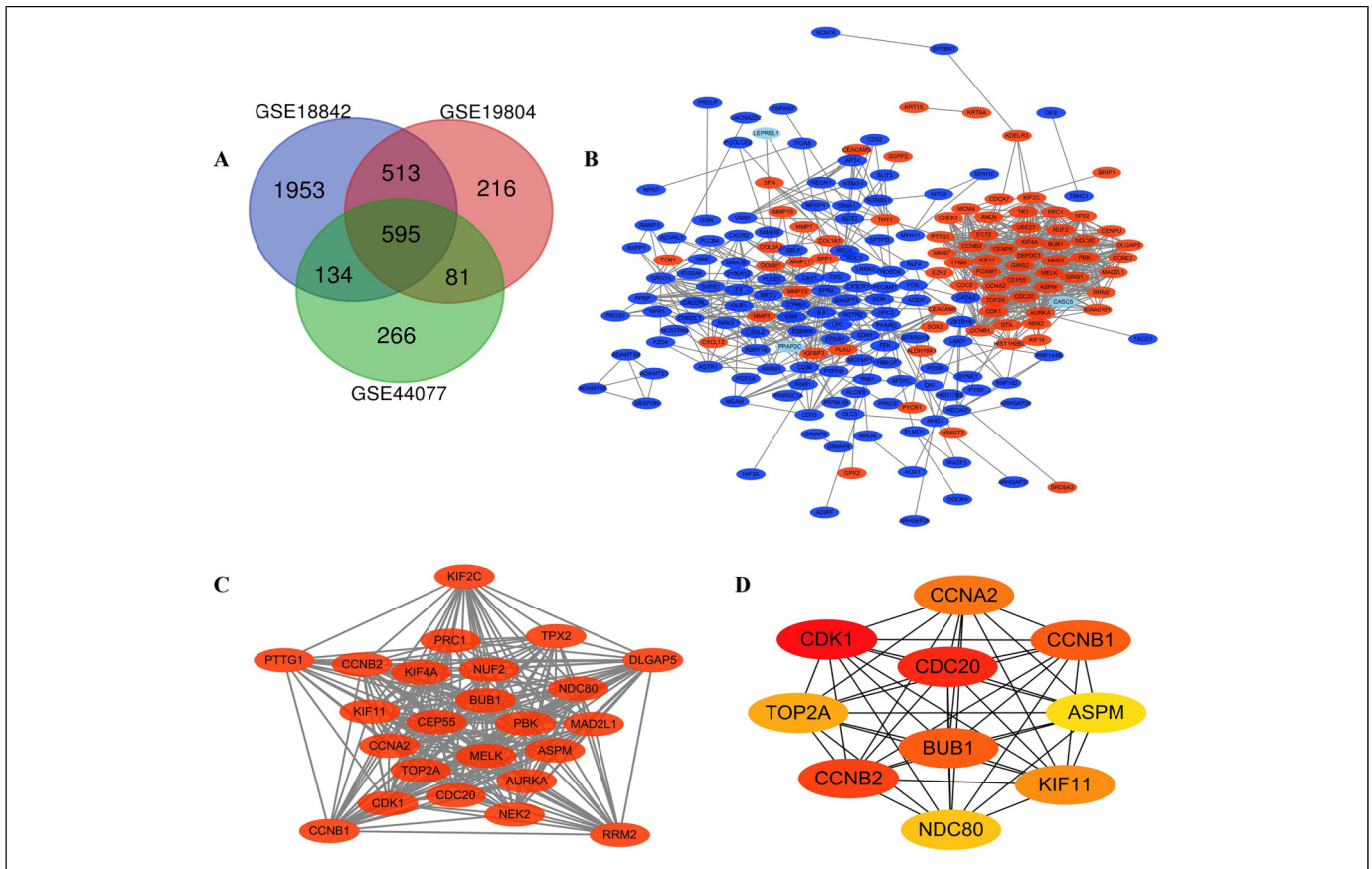


**Figure 1.** Venn diagram, protein-protein interaction (PPI) network, the most significant module, and the top 10 highest scoring nodes of differentially expressed genes (DEGs). (A) DEG identification in three gene expression profile datasets (GSE18842, GSE44077, and GSE19804). In total, 594 DEGs were identified. (B) A PPI network was generated using Cytoscape (combined score  $\geq 0.9$ ). (C) The significant module obtained from the PPI network contained 24 nodes and 256 edges. (D) The interaction network of the 10 nodes with the highest screening scores. Upregulated genes are marked in dark red; downregulated genes are marked in dark blue. The red, orange, and yellow nodes represented the top 10 hub genes in the network.

the PPI network, with the following parameters: cut-off degree = 2, cut-off node score = 0.2, K-core = 2, and maximum depth = 100. Functional annotation of DEGs in the identified module was investigated with DAVID. The cut-off criterion was set to a  $P$  value less than 0.05.

The Kaplan–Meier Plotter database (<http://kmplot.com/analysis/index.php?p=service&cancer=lung>), which provides information on the relationships of more than 54 000 genes (mRNAs, microRNAs, and proteins) with survival rates in 21 cancer types,<sup>22</sup> was used to investigate whether the top 10 hub genes were related to overall survival in patients with NSCLC. We also assessed relationships according to histological type, including adenocarcinoma (LUAD) and squamous cell carcinoma (LUSC). Subsequently, we analyzed the association of overall survival rate with hub genes according to treatment strategies in order to compare the prognostic significance of hub genes under different treatment regimens. The selection criteria were as follows: hazard ratio (HR) within the 95% confidence interval (CI) and log-rank  $P$  value less than .05.

Next, we used the Cytoscape plug-in CytoHubba to identify hub genes, subnets of complex networks, and central

elements in the network. The Biological Networks Gene Oncology Tool (BiNGO; version 3.0.3) plug-in in Cytoscape was used to analyze and visualize the biological processes (BPs) associated with the hub genes. The Oncomine database (<http://www.oncomine.org>) was used to compare the mRNA expression levels of hub genes between lung cancer tissues and normal control tissues and between different types of lung cancer. Data were collected from all related datasets.

Gene Expression Profiling Interactive Analysis (GEPIA; <http://gepia.cancer-pku.cn/index.html>) is a new web-based interactive analysis and visualization tool based on The Cancer Genome Atlas (TCGA) database and genotype tissue expression.<sup>23</sup> To further verify the 10 hub genes identified from the PPI network, differences in gene expression between LUSC, LUAD, and adjacent lung tissues were mapped in TCGA database and GTEx database using the GEPIA web tool Box Plots. The patient data were grouped according to the results per million reads (TPM).  $\log_2(\text{TPM} + 1)$  was used as the logarithmic scale, and the criteria were as follows:  $|\log_2\text{FC}| > 1$  and  $p < .01$ .

**Table 1.** GO Function Annotation of uDEGs and dDEGs Associated With NSCLC (top five).

Category	Term	Count	%	P-value
<b>uDEGs</b>				
GOTERM_BP_DIRECT	GO:0007067~mitotic nuclear division	22	0.07753304	7.26E-14
GOTERM_BP_DIRECT	GO:0051301~cell division	23	0.081057269	7.34E-12
GOTERM_BP_DIRECT	GO:0030574~collagen catabolic process	10	0.035242291	1.47E-08
GOTERM_BP_DIRECT	GO:0007062~sister chromatid cohesion	11	0.03876652	8.61E-08
GOTERM_BP_DIRECT	GO:0008283~cell proliferation	17	0.059911894	9.22E-07
GOTERM_CC_DIRECT	GO:0030496~midbody	12	0.042290749	3.90E-08
GOTERM_CC_DIRECT	GO:0000777~condensed chromosome kinetochore	10	0.035242291	1.31E-07
GOTERM_CC_DIRECT	GO:0005819~spindle	10	0.035242291	2.20E-06
GOTERM_CC_DIRECT	GO:0000922~spindle pole	9	0.031718062	9.04E-06
GOTERM_CC_DIRECT	GO:0000776~kinetochore	8	0.028193833	1.14E-05
GOTERM_MF_DIRECT	GO:0004222~metalloendopeptidase activity	12	0.042290749	1.37E-08
GOTERM_MF_DIRECT	GO:0004252~serine-type endopeptidase activity	15	0.052863436	2.15E-07
GOTERM_MF_DIRECT	GO:0019901~protein kinase binding	14	0.049339207	8.48E-05
GOTERM_MF_DIRECT	GO:0003777~microtubule motor activity	7	0.024669604	1.32E-04
GOTERM_MF_DIRECT	GO:0042802~identical protein binding	19	0.066960352	3.92E-04
<b>dDEGs</b>				
GOTERM_BP_DIRECT	GO:0007155~cell adhesion	38	0.059311981	9.75E-12
GOTERM_BP_DIRECT	GO:0001525~angiogenesis	23	0.035899357	4.70E-09
GOTERM_BP_DIRECT	GO:0007166~cell surface receptor signaling pathway	25	0.03902104	9.87E-09
GOTERM_BP_DIRECT	GO:0001570~vasculogenesis	10	0.015608416	3.37E-06
GOTERM_BP_DIRECT	GO:0045766~positive regulation of angiogenesis	13	0.020290941	8.80E-06
GOTERM_CC_DIRECT	GO:0005578~proteinaceous extracellular matrix	30	0.046825248	1.58E-12
GOTERM_CC_DIRECT	GO:0005886~plasma membrane	146	0.227882874	3.56E-10
GOTERM_CC_DIRECT	GO:0005887~integral component of plasma membrane	68	0.106137229	1.70E-09
GOTERM_CC_DIRECT	GO:0016021~integral component of membrane	161	0.251295499	3.09E-07
GOTERM_CC_DIRECT	GO:0045121~membrane raft	19	0.029655991	7.41E-07
GOTERM_MF_DIRECT	GO:0008201~heparin binding	17	0.026534307	2.62E-07
GOTERM_MF_DIRECT	GO:0005509~calcium ion binding	38	0.059311981	4.32E-07
GOTERM_MF_DIRECT	GO:0030246~carbohydrate binding	16	0.024973466	1.72E-05
GOTERM_MF_DIRECT	GO:0005178~integrin binding	11	0.017169258	7.15E-05
GOTERM_MF_DIRECT	GO:0003779~actin binding	18	0.028095149	8.51E-05

Abbreviations: dDEGs: downregulated differentially expressed gene; GO: Gene Ontology; NSCLC: non-small cell lung cancer; uDEGs: upregulated differentially expressed genes.

**Table 2.** KEGG Pathway Analysis of DEGs Associated With NSCLC.

Category	Term	Count	%	P-value
<b>uDEGs</b>				
KEGG_PATHWAY	hsa04110:Cell cycle	15	0.052863436	1.42E-10
KEGG_PATHWAY	hsa04115:p53 signaling pathway	8	0.028193833	1.29E-05
KEGG_PATHWAY	hsa04114:Oocyte meiosis	9	0.031718062	4.72E-05
KEGG_PATHWAY	hsa04914:Progesterone-mediated oocyte maturation	6	0.021145374	.003663974
KEGG_PATHWAY	hsa04512:ECM-receptor interaction	6	0.021145374	.003663974
<b>dDEGs</b>				
KEGG_PATHWAY	hsa04514:Cell adhesion molecules (CAMs)	12	0.018730099	.001027649
KEGG_PATHWAY	hsa05144:Malaria	7	0.010925891	.001487862
KEGG_PATHWAY	hsa04270:Vascular smooth muscle contraction	10	0.015608416	.003069086
KEGG_PATHWAY	hsa03320:PPAR signaling pathway	7	0.010925891	.007259593
KEGG_PATHWAY	hsa04610:Complement and coagulation cascades	7	0.010925891	.00836134

Abbreviations: DEGs: differentially expressed genes; dDEGs: downregulated differentially expressed genes; KEGG: Kyoto Encyclopedia of Genes and Genomes; NSCLC: non-small cell lung cancer; uDEGs: upregulated differentially expressed genes.

The Human Protein Atlas (THPA), which maps all human proteins in cells, tissues and organs by integrating various omics technologies (including antibody-based imaging, mass spectrometry-based proteomics, transcriptomics, and systems).<sup>24</sup>, was used to assess protein-based differences between NSCLC and normal tissues. First, we downloaded the histological section images and corresponding information on overexpressed hub genes from normal bronchial

**Table 3.** Top 10 in Network Ranked by Degree Method.

Rank	Name	Type	Score
1	<i>CDK1</i>	up	42
2	<i>CDC20</i>	up	40
3	<i>CCNB2</i>	up	35
4	<i>BUB1</i>	up	34
4	<i>CCNB1</i>	up	34
6	<i>CCNA2</i>	up	33
7	<i>KIF11</i>	up	32
8	<i>TOP2A</i>	up	31
9	<i>NDC80</i>	up	30
10	<i>ASPM</i>	up	29

respiratory tract epithelial tissues and lung cancer tissues obtained by immunohistochemistry from THPA. Because some antibody staining may be inconsistent, the detection results were reported as low, medium, or high according to the staining intensity and score of the stained cells. We then performed Mann–Whitney U tests using SPSS 23.0 software to compare the antibody staining levels of hub genes between normal lung tissues and bronchial epithelial tissues. The cut-off *P* value was set to .05.

All cell lines were obtained from Professor Haidan Liu (Changsha). A549 human NSCLC cells (epidermal growth factor receptor wild type) and HBE normal immortalized lung epithelial cells were purchased from American Type Culture Collection (ATCC). The cells were cultured in a humidified incubator at 37°C with 5% CO<sub>2</sub> according to ATCC protocols. A549 cells were subjected to mycoplasma analysis and were cytogenetically tested and authenticated before being frozen. HBE cells were maintained in Dulbecco's modified Eagle's medium (Thermo Fisher Scientific) supplemented with 10% fetal bovine serum (FBS; Biological Industries) and 1% antibiotics. A549 cells were maintained in RPMI1640 medium (Thermo Fisher Scientific) supplemented with 10% FBS (Biological Industries) and 1% antibiotics.

For quantitative real-time polymerase chain reaction (qPCR), HBE and A549 cells were seeded in 100-mm Petri dishes and grown for 1 day at 37 °C in an atmosphere containing 5% CO<sub>2</sub>. After 48 h, total RNA was extracted using a GeneJET RNA Purification Kit (Thermo Fisher Scientific) according to the manufacturer's instructions. Additionally, a RevertAid First Strand cDNA Synthesis Kit (Thermo Fisher Scientific) was used to synthesize cDNA based on the manufacturer's recommendations. qPCR was then performed in a Thermo 9700 Fast Real-time PCR system using PowerUp SYBR Green Master Mix (Thermo Fisher Scientific). The qPCR reaction conditions were: UDG enzyme activation, 50[?] for 2 min, a hold; pre-denaturation, 95[?] for 2 min, a hold; denaturation, 95[?] for 3 s and annealing and extension, 60[?] for 30 s, 40 cycles. The melting curve selects the default setting. The reaction system used a 10ul reaction system, and the sample amount of cDNA is 10 ng per reaction. The primers used were as follows: *ARF5*-F, 5'-ATCTGTTTCACAGT

CTGGGACG-3'; *ARF5*-R, 5'-CCTGCTTGTGGCAAAT ACC-3'; *CDC20*-F, 5'-AGACATTCACCCAGCATCAAG-3'; *CDC20*-R, 5'-GAGATGAGCTCCTTGTAATGGG-3'; *CCN B1*-F, 5'-GGCTTTCTCTGATGTAATCTTGC-3'; *CCN B1*-R, 5'-GTATTTTGGTCTGACTGCTTGC-3'; *TOP2A*-F, 5'-ATCTAAACCTCTTGCAGCCC-3'; *TOP2A*-R, 5'-GCA CCATTTATCAGCACCATG-3'; *CCNB2*-F, 5'-ACCTA CTGCTTCTGTCAAACC-3'; *CCNB2*-R, 5'-TGTCTCTCG ATTTTGCAGAGC-3'; *CCNA2*-F, 5'-CCTTTTCATTTA GCACTCTACACAG-3'; *CCNA2*-R, 5'-CCAGGGTATATCC AGTCTTTTCG-3'; *KIF11*-F, 5'-ACCTCATGTTCCTTATCG AGAATC-3'; *KIF11*-R, 5'-GCATATTCCAATGTACTCAG AGTTTC-3'. *ARF5* was used as an internal control,<sup>25</sup> and fold changes in mRNA levels were determined using the 2<sup>-ΔΔCT</sup> method.

All data were presented as means ± standard deviations. GraphPad Prism 8.0 (GraphPad Software) and SPSS software were used for all statistical analyses. Two-tailed Student's *t*-tests were used to assess the significance of differences between the two groups. Unless otherwise stated, results with *P* values less than .05 were considered statistically significant.

## Results

### Identification of Differentially Expressed Cells in Non-Small Cell Lung Cancer

According to GEO2R analysis, after standardizing the chip data, DEGs (4642 in GSE18842, 1960 in GSE19804, and 1235 in GSE44077) were identified. Among these DEGs, the three datasets together contained 594 genes, as demonstrated by Venn diagram analysis in the Bioinformatics & Evolutionary Genomics platform (Figure 1A and Supplementary Table S4). We matched the log<sub>2</sub>FC values of three independent datasets to DEGs and found that 177 uDEGs and 417 dDEGs were identified between NSCLC and normal tissues in all three independent datasets.

### Gene Ontology Functional Pathways and Analysis of Differentially Expressed Genes

GO analyses showed that uDEGS were mainly enriched in mitotic nuclear division, whereas dDEGs were mainly enriched in cell adhesion (Supplementary Table S5). Furthermore, cell component (CC) analysis indicated that most of the uDEGs were located in the midbody, whereas the dDEGs were mainly distributed in the proteinaceous extracellular matrix. Additionally, according to molecular function (MF) analysis, uDEGs were significantly associated with metalloendopeptidase activity, whereas dDEGs were associated with heparin binding (Table 1). KEGG pathway analysis suggested that most uDEGs were mainly involved in the BPs of the cell cycle, whereas most dDEGs were involved in cell adhesion (Table 2).

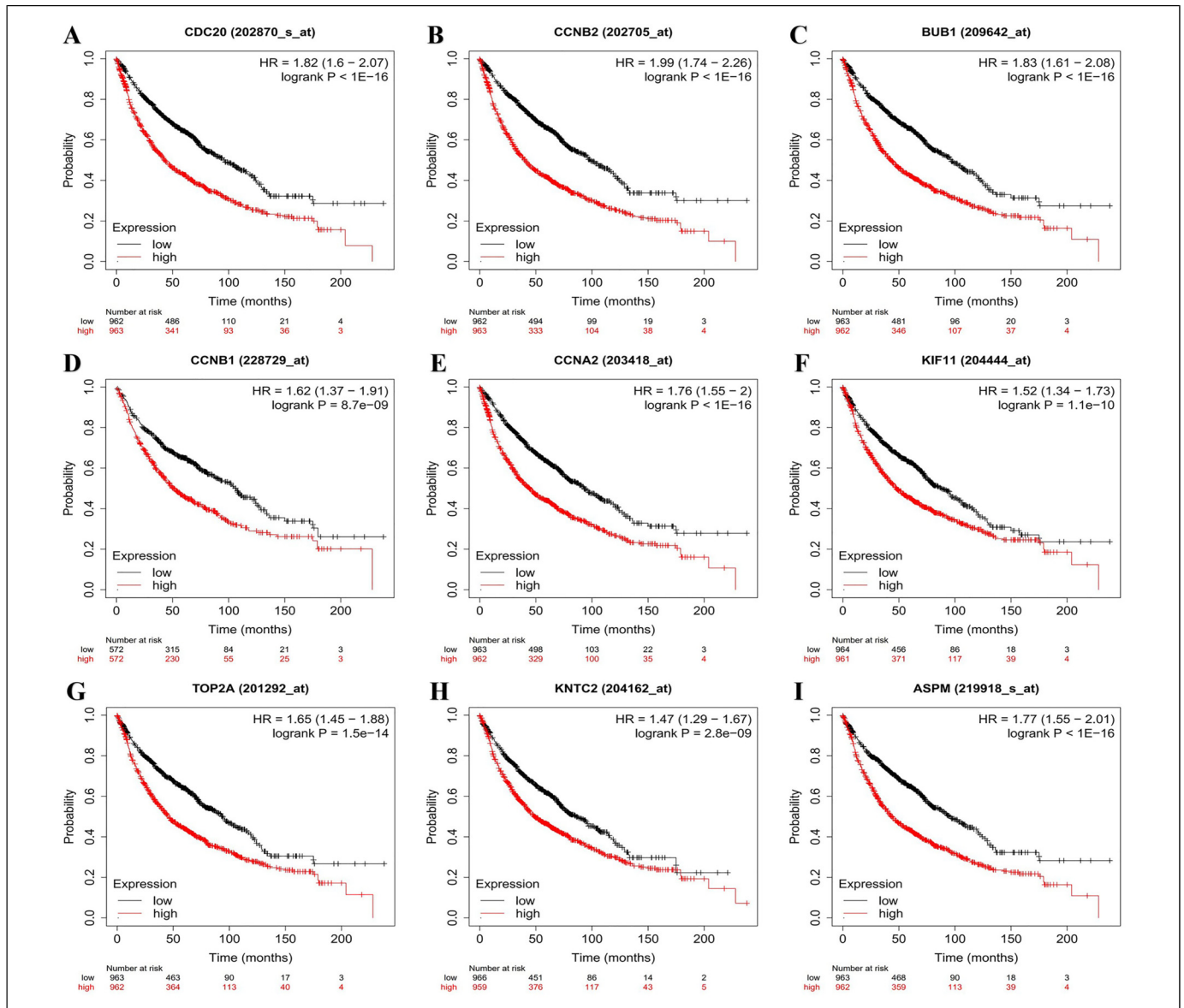


**Figure 2. Association of hub genes with overall survival rates.** Kaplan–Meier Plotter was used to evaluate overall survival rates based high or low expression of (A) *CDC20*, (B) *CCNB2*, (C) *BUB1*, (D) *CCNB1*, (E) *CCNA2*, (F) *KIF11*, (G) *TOP2A*, (H) *NDC80*, and (I) *ASPM* in patients with non-small cell lung cancer (NSCLC).

### Protein-Protein Interaction Network Construction and Analysis of Modules

Next, we constructed a PPI network of DEGs. The PPI network contained 202 nodes and 743 edges, including 75 uDEGs and 124 DEGs (Figure 1B). According to the selection conditions, 19 sets of datasets were obtained, and the one with the highest cluster score was selected for subsequent in-depth analyses. The PPI network with the highest cluster score calculated using the MCODE plug-in generated 24 nodes and 256 edge-related modules, with a cluster score of 22.261 (Figure 1C and Supplementary Table S6). The top 10 highest scoring nodes, including *CDC20*, *CCNB2*, *BUB1*, *CCNB1*, *CCNA2*, *KIF11*, *TOP2A*, *NDC80*, *ASPM*, *CDK1*, were then evaluated using the Cytohubba plug-in (Table 3) and were used to build an interaction

network in MCODE (Figure 1D). In addition to the 10 genes described above, other nodes in the module included *KIF4A*, *PRC1*, *RRM2*, *PTTG1*, *MELK*, *TPX2*, *AURKA*, *CEP55*, *MAD2L1*, *NEK2*, *NUF2*, *DLGAP5*, *KIF2C*, and *PBK*. The expression levels of all genes in the module were upregulated.

### Hub Gene Selection and Survival Analysis

Using the Kaplan–Meier Plotter online database, we evaluated the relationships between nine of the 10 hub genes (excluding *CDK1*) and overall survival rates (Figure 2). The results indicated that the overexpressed hub genes were related to unfavorable overall survival in patients with NSCLC, as follows: *CDC20* (HR = 1.82 [95% CI: 1.6-2.07], log-rank  $P < 1e-16$ ), *CCNB2* (HR = 1.99 [95% CI: 1.74-2.26], log-rank  $P <$

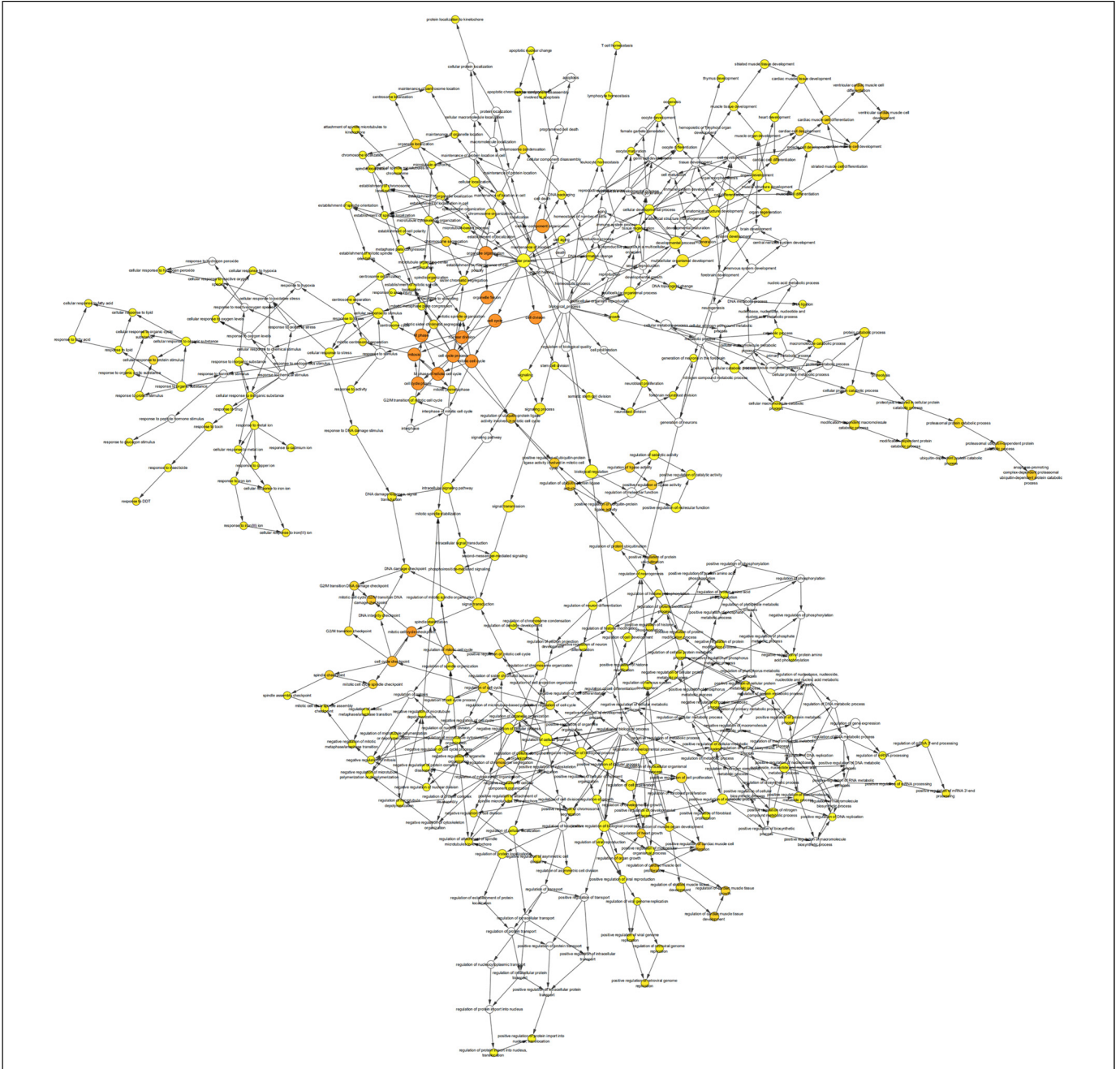


**Figure 3. Analysis of biological processes (BPs) enriched in hub genes.** BiNGO was used to assess the BPs enriched in hub genes. The color depth of the node reflects the corrected  $P$  value.

Abbreviation: BiNGO: Biological Networks Gene Oncology Tool.

$1e-16$ ), *BUB1* (HR = 1.77 [95% CI: 1.55-2.01], log-rank  $P = 1e-16$ ), *CCNB1* [HR = 1.62 [95% CI: 1.37-1.91], log-rank  $P = 8.7e-09$ ], *CCNA2* [HR = 1.76 [95% CI: 1.55-2], log-rank  $P < 1e-16$ ], *KIF11* [HR = 1.52 [95% CI: 1.34-1.73], log-rank  $P = 1.1e-10$ ], *TOP2A* [HR = 1.65 [95% CI: 1.45-1.88], log-rank  $P = 1.5e-14$ ], *NDC80* [HR = 1.47 [95% CI: 1.29-1.67], log-rank  $P = 2.8e-09$ ], *ASPM* [HR = 1.77 [95% CI: 1.55-2.01], log-rank  $P < 1e-16$ ]. Analysis of the BPs enriched for the nine hub genes is shown in Figure 3. Furthermore, using the OncoPrint database, we confirmed

that the nine hub genes were upregulated in NSCLC tissues compared with control tissues and cells [all  $P < 1e-4$ ; Figure 4].

### Verification of hub Genes Using Gene Expression Profiling Interactive Analysis

To determine the reliability of DEGs identified from GSE18842, GSE19804, and GSE44077, we used GEPIA for the assessment of hub gene expression levels in LUAD, LUSC, and normal lung tissues reported in the TCGA database.

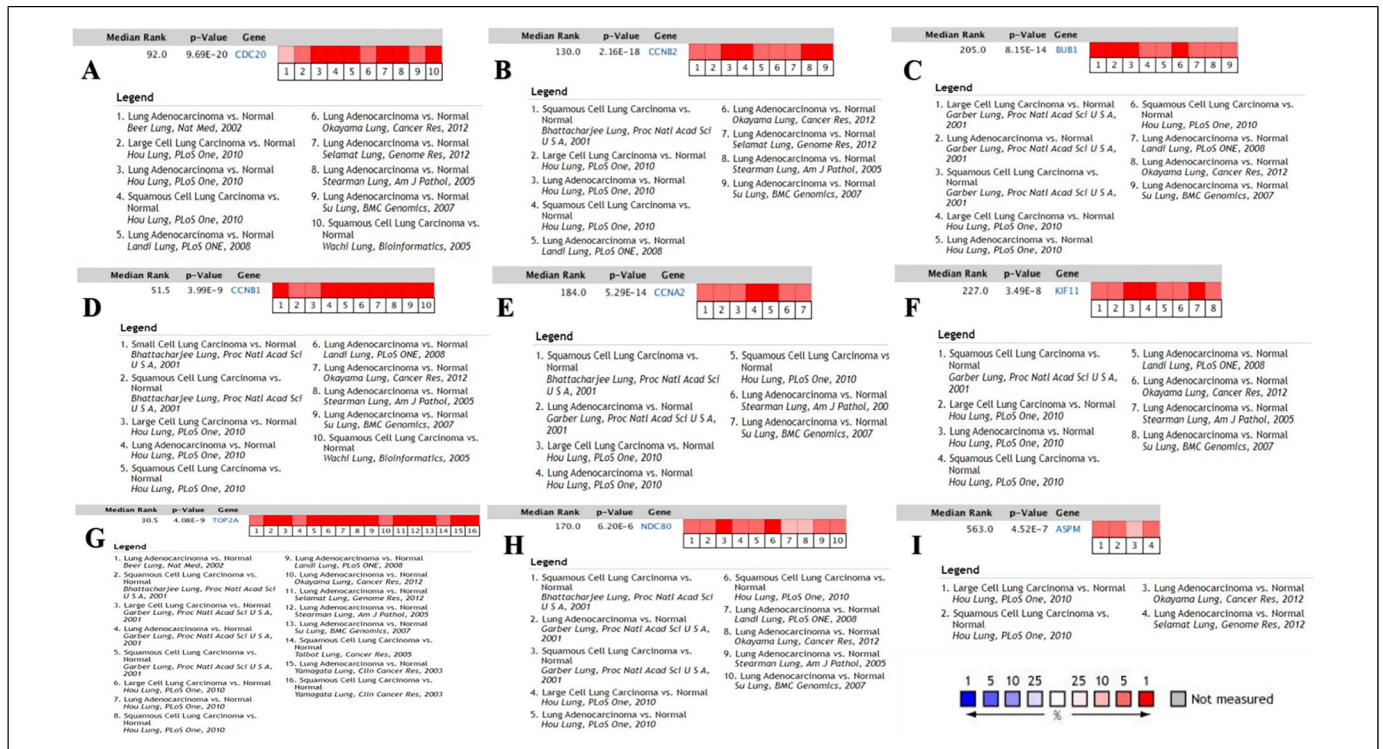


**Figure 4. Evaluation of gene expression in cancer tissues and normal tissues using OncoPrint.** OncoPrint was used to evaluate (A) *CDC20*, (B) *CCNB2*, (C) *BUB1*, (D) *CCNB1*, (E) *CCNA2*, (F) *KIF11*, (G) *TOP2A*, (H) *NDC80*, and (I) *ASPM* expression in cancer tissues versus normal tissues.

Consistent with the results of bioinformatics analysis of GEO data, the nine hub genes were identified, and their expression levels were found to be significantly increased (Figure 5).

### Verification of hub Genes Based on Proteomics Analysis

Next, we used immunohistochemical images of proteins from THPA database to further verify the relevance of six hub genes in lung cancer tissues (Figure 6A). *CDC20* (18/21), *CCNB2* (17/26), *CCNB1* (29/35), *CCNA2* (10/11), *KIF11* (31/33), and *TOP2A* (34/34) had high positive staining rates; however, only *CDC20* ( $P = .000014$ ), *CCNB1* ( $P = .000021$ ), and *TOP2A* ( $P = .000013$ ) were compared by Mann–Whitney U test using normal lung cells, bronchial epithelial cells, and lung cancer tissues. The results showed statistically significant differences in the protein levels of these hub genes (Figure 6B), suggesting potential applications as biomarkers in the diagnosis of NSCLC.

### Verification of hub Gene Upregulation by Quantitative Polymerase Chain Reaction

We then used qPCR to analyze the expression levels of the six hub genes (including three screened out and three unverified) in A549 and HBE cells. Consistent with bioinformatics analysis data, *CCNB1*, *CCNB2*, *CCNA2*, and *TOP2A* were significantly

upregulated in A549 cells compared with that in HBE cells (Figure 7 and Supplementary Tables S7–S9).

### Analysis of hub Gene Expression Levels in Different Types of Non-Small Cell Lung Cancer

The OncoPrint database was used to analyze differences in the expression level of four hub genes in different types of NSCLCs reported in Hou's dataset.<sup>26</sup> The analytical results showed that compared with normal control tissues, gene expression levels were elevated in all types of NSCLCs, consistent with the verification results. Moreover, in a comparison between large cell lung carcinoma, LUAD, and LUSC, the expression levels of all four hub genes were highest in large cell lung carcinoma, followed by LUSC and then LUAD (Figure 8).

### Analysis of the Relationships Between Overall Survival and hub Gene Expression Based on Treatment Strategies in Patients With Non-Small Cell Lung Cancer

Finally, we used Kaplan–Meier Plotter online database to assess the relationships between overall survival rates and hub gene expression according to treatment strategies. As shown in Figure 9A, F, K, and P, the four hub genes



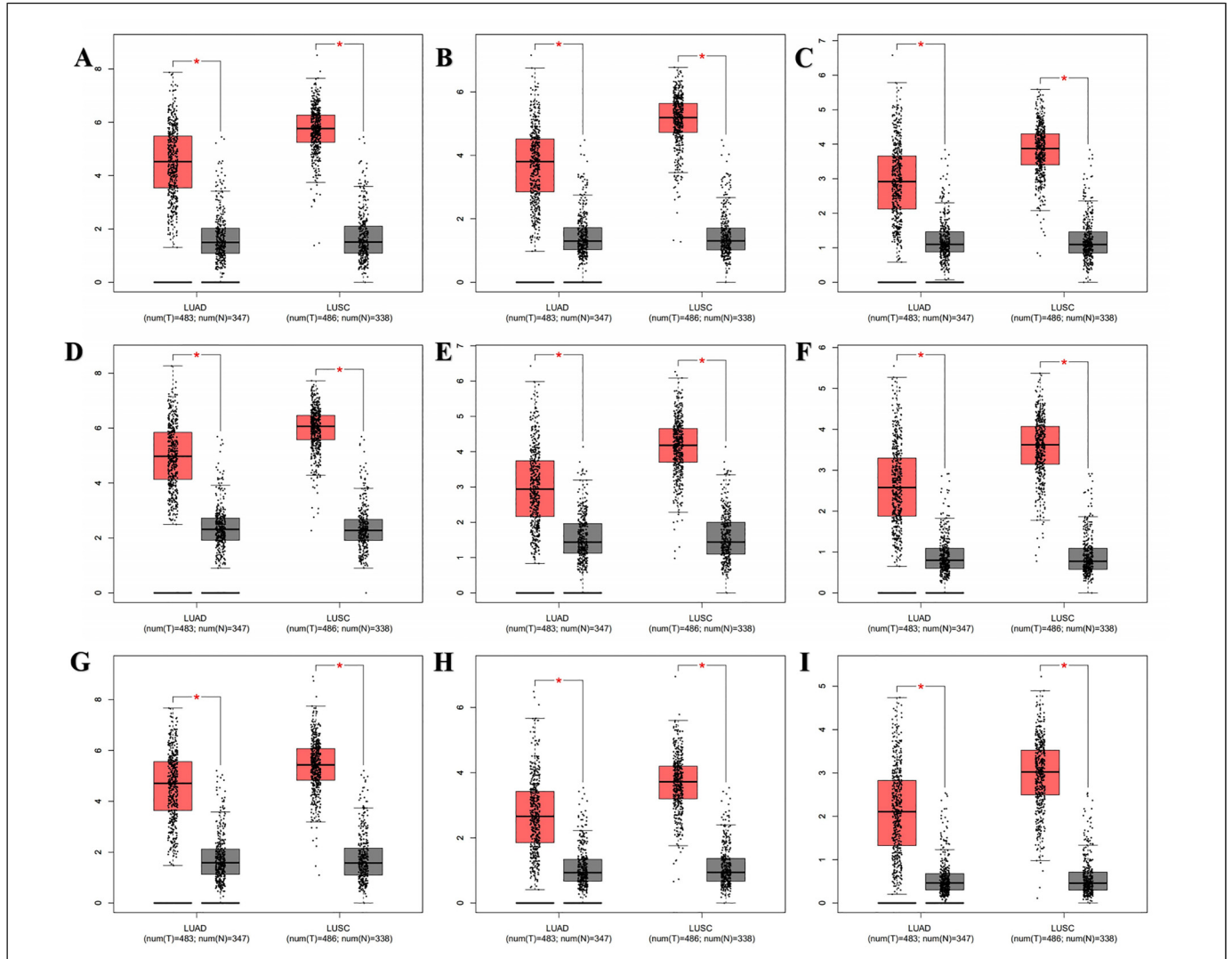


**Figure 5. Expression levels of the nine hub genes.** Heat map showing the expression levels of nine hub genes (*CDC20*, *CCNB2*, *BUB1*, *CCNB1*, *CCNA2*, *KIF11*, *TOP2A*, *NDC80*, and *ASPM*) in LUAD, LUSC, and normal lung tissues based on TCGA data analyzed using the GEPIA web tool. T represents LUAD or LUSC tumor tissues, and N represents normal lung tissues.

Abbreviations: GEPIA: Gene Expression Profiling Interactive Analysis; LUAD: lung adenocarcinoma; LUSC: lung squamous cell carcinoma; TCGA: The Cancer Genome Atlas.

significantly predicted overall survival for patients who underwent surgical resection only. Moreover, as shown in Figure 9B, G, L, and Q, among the four hub genes, only *CCNB1* could predict overall survival in patients who underwent chemotherapy; however, the median survival time was lower for patients categorized as having high expression of the four hub genes than for patients categorized as having low expression. We also found that the four hub genes significantly predicted overall survival in patients who were not treated with chemotherapy (Figure 9C, H, M, and R), whereas no significant prediction ability was observed in patients who underwent radiotherapy (Figure 9D, I, N, and S), although the median survival time in patients with high expression was still shorter than that in patients with low hub gene expression. Additionally, in patients who were not

treated with radiotherapy, *CCNB1* and *CCNA2* significantly predicted overall survival, and patients with high expression of the other two hub genes also had lower median survival times (Figure 9E, J, O, and T).

## Discussion

Lung cancer is a major threat to human health, and although targeted immunotherapies have improved the quality of life of many patients, clinical outcomes in patients with NSCLC remain poor. To date, the pathogenic mechanisms of NSCLC have not been fully elucidated; however, multiple genes and pathways are known to be involved, resulting in complex biological behaviors. Accordingly, improving our understanding of the molecular

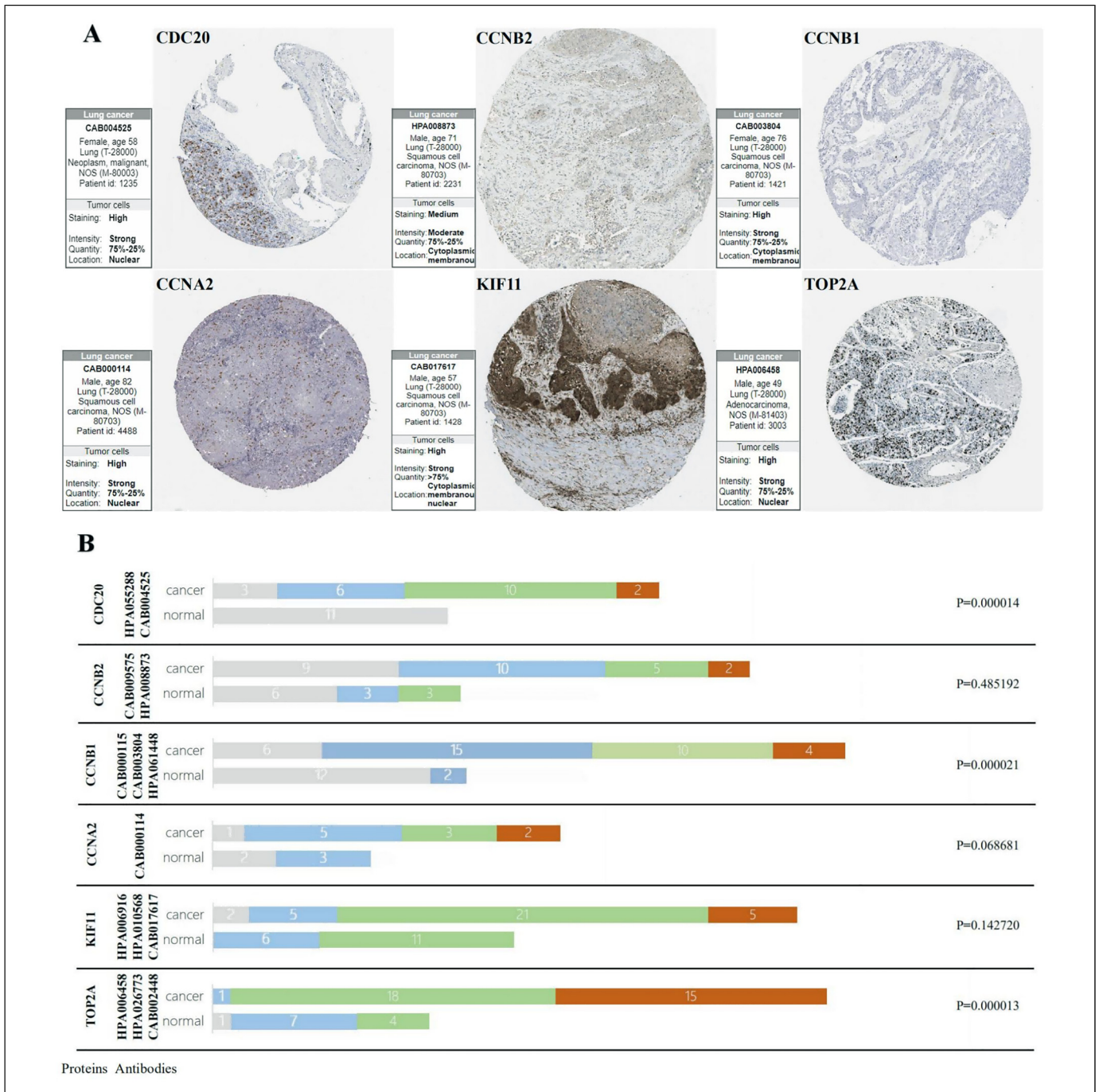


**Figure 6. Verification of the protein expression levels of hub genes.** (A) Immunohistochemistry images of six hub genes were obtained from <https://www.proteinatlas.org/ENSG00000117399-CDC20/pathology/lung+cancer#ihc> (CDC20), <https://www.proteinatlas.org/ENSG00000157456-CCNB2/pathology/lung+cancer#ihc> (CCNB2), <https://www.proteinatlas.org/ENSG00000134057-CCNB1/pathology/lung+cancer#ihc> (CCNB1), <https://www.proteinatlas.org/ENSG00000145386-CCNA2/pathology/lung+cancer#ihc> (CCNA2), <https://www.proteinatlas.org/ENSG00000138160-KIF11/pathology/lung+cancer#ihc> (KIF11), and <https://www.proteinatlas.org/ENSG00000131747-TOP2A/pathology/lung+cancer#ihc> (TOP2A) in THPA. (B) The antibodies used targeted CDC20 (HPA055288 and CAB004525), CCNB2 (CAB009575 and HPA008873), CCNB1 (CAB000115, CAB003804, and HPA061448), CCNA2 (CAB000114), KIF11 (HPA006916, HPA010568, and CAB017617), and TOP2A (HPA006458, HPA026773, and CAB002448). Mann–Whitney U tests were used for assessing significance, with a cut-off *P* value of .05. Abbreviation: THPA: The Human Protein Atlas.

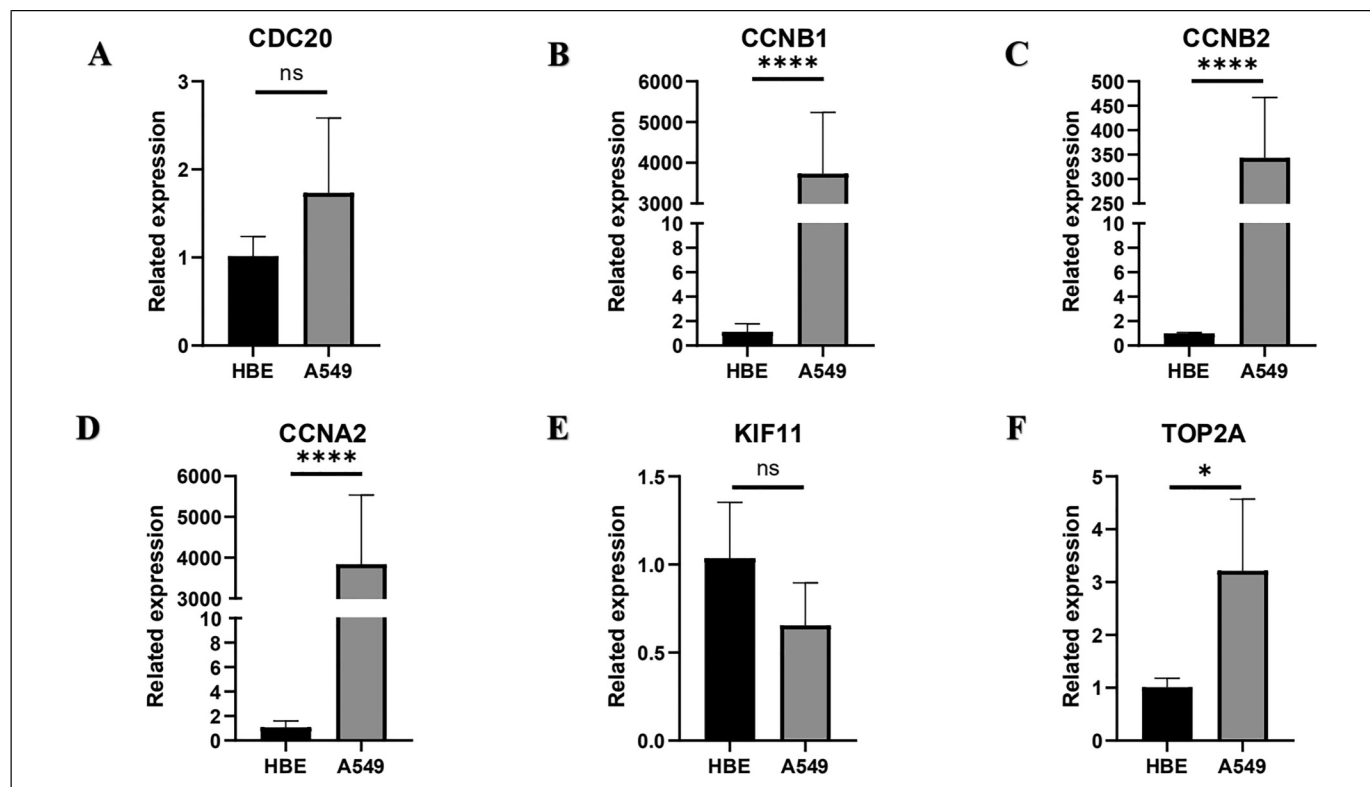


**Figure 7. Expression levels of six hub genes in A549 and HBE cells.** Expression levels were verified using RT-qPCR. (A) *CDC20*, (B) *CCNB1*, (C) *CCNB2*, (D) *CCNA2*, (E) *KIF11*, *TOP2A*. \* $P < .05$ , \*\* $P < .01$ , \*\*\* $P < .001$ , \*\*\*\* $P < .0001$ , ns: not significant.

mechanisms of NSCLC, particularly using genomics, transcriptomics, proteomics, and metabolomics analyses, is expected to lead to the development of better diagnostic and therapeutic strategies based on identification of novel biomarkers.<sup>27</sup>

In this study, we selected 594 DEGs, including 177 uDEGs and 417 dDEGs, and found that the uDEGs were primarily involved in mitotic nuclear division, cell cycle, p53 signaling, oocyte meiosis, progesterone-mediated oocyte maturation, and extracellular matrix-receptor interactions, whereas the dDEGs were mainly enriched in cell adhesion, malaria, vascular smooth muscle contraction, peroxisome proliferator-activated receptor signaling, complement molecules, and coagulation cascade. Thus, this functional enrichment analysis provided insights into the signaling pathways involved in the occurrence and development of NSCLC. In normal and tumor cells, mitotic nuclear division, cell cycle, and meiotic division of oocytes are known to be important cellular processes,<sup>28</sup> and key tumor-related genes usually modulate tumor progression by regulating these cellular processes.<sup>29</sup> Furthermore, some studies have shown that cell adhesion molecules play crucial roles in tumor development,<sup>30</sup> consistent with our current results. Thus, although the specific mechanisms of disease progression are still not clearly defined, the signaling pathways identified above were confirmed to be related to NSCLC.

Next, we generated a PPI network of the DEGs. The top 10 genes and one relevant module extracted from the PPI network

were all upregulated and survival analysis showed that nine of these genes (*CDC20*, *CCNB2*, *BUB1*, *CCNB1*, *CCNA2*, *KIF11*, *TOP2A*, *NDC80*, and *ASPM*) were significantly correlated with overall survival in patients with NSCLC. We further confirmed that *CCNB1*, *CCNB2*, *CCNA2*, and *TOP2A* were upregulated in NSCLC cells compared with normal lung cells and demonstrated that these four hub genes showed higher prognostic value in patients who underwent surgery and in patients who had not received chemotherapy. Furthermore, *CCNB1* and *CCNA2* had good prognostic value in patients who had not received radiotherapy. Overall, these findings suggested that the four hub genes may have applications as promising biomarkers in NSCLC.

*CCNB1* encodes the regulatory protein cyclin B1, which is involved in mitosis. The gene product can interact with p34 (*CDC2*) to form a maturation promoting factor and has been shown to modulate the G<sub>2</sub>/M transition phase of the cell cycle. Moreover, *CCNB1* has been shown to act as a potential diagnostic marker for rhabdomyosarcoma and estrogen receptor (ER)-positive breast cancer.<sup>31</sup> *CCNB1* exerts carcinogenic effects in colorectal cancer cells and may be an effective target in the development of new treatments for colorectal cancer.<sup>32</sup> Researchers have also shown that overexpression of G<sub>2</sub> and S phase-expressed-1 promotes cell proliferation, migration, and invasion by regulating *CCNB1* and other pathways and predicts poor outcomes in patients with bladder cancer.<sup>33</sup> In a study of NSCLC, Arora et al. discovered that a network

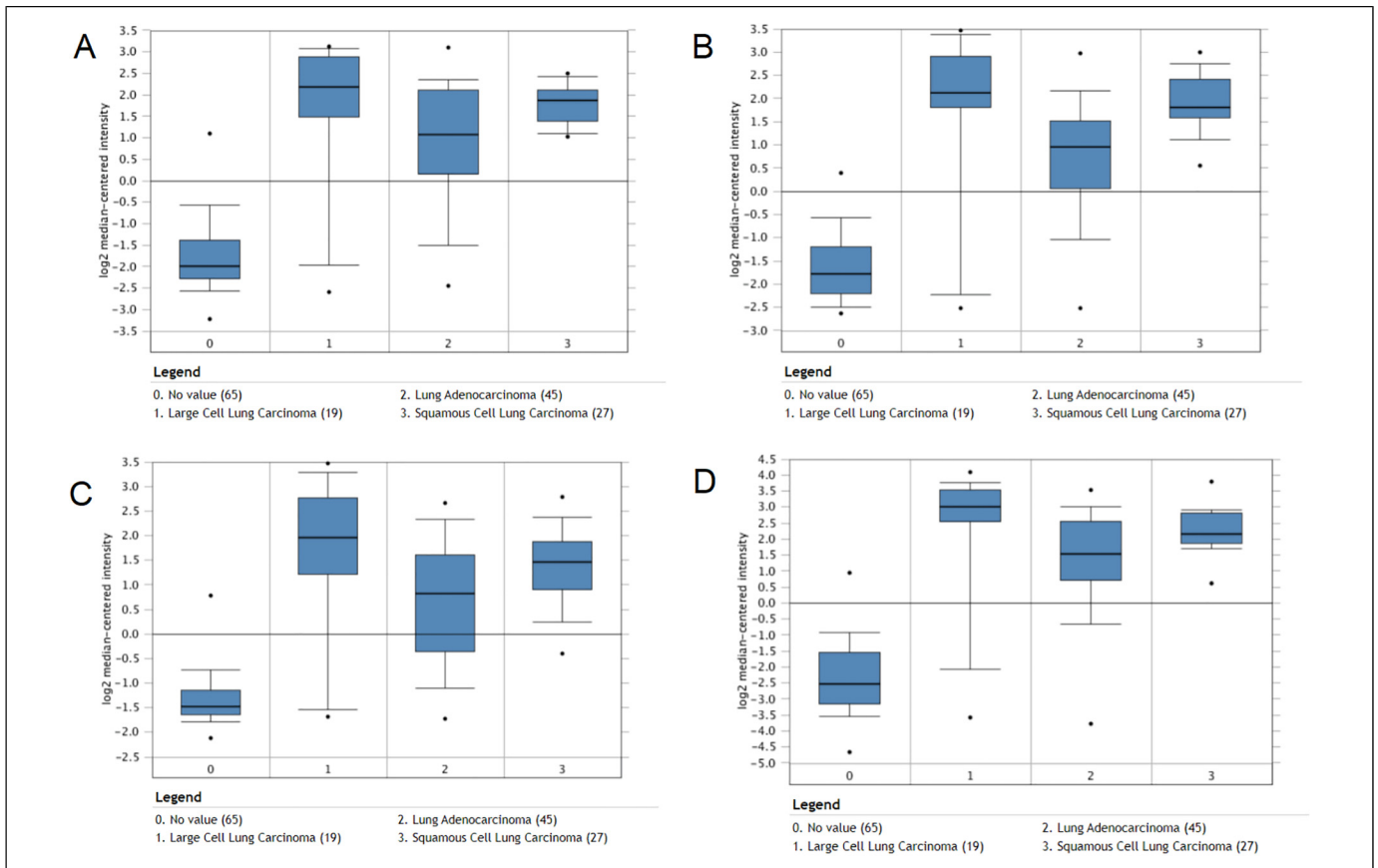


**Figure 8. Predictive ability of hub genes in distinguishing among different types of non-small cell lung cancer (NSCLC) tissues.** Data were evaluated using Oncomine. (A) *CCNB1*, (B) *CCNB2*, (C) *CCNA2*, and (D) *TOP2A*.

composed of *miR-20b-5p*, *CCNB1*, *HMG2*, and *E2F7* plays important roles in the development and progression of NSCLC,<sup>34</sup> suggesting that these targets may be effective prognostic biomarkers and may facilitate the development of novel treatments for NSCLC. Indeed, the cell cycle and immune surveillance mechanisms can be targeted through *HMG2* and *E2F7*, and the *CCNB1* gene may be a crucial component in various cancers.

Cyclin B2, encoded by the *CCNB2* gene, is a type B cyclin that has been shown to be upregulated in human cancer. *CCNB2* is vital for controlling the cell cycle during the  $G_2/M$  transition (mitosis) via modulation of p34 (CDC2). The subcellular localization of cyclins B1 and B2 differs; *CCNB2* is mainly localized to the Golgi apparatus, whereas cyclin B1 is expressed near microtubules. Because *CCNB2* also binds to transforming growth factor (TGF)  $\beta$ RII, *CCNB2/CDC2* may have essential roles in TGF- $\beta$ -mediated cell cycle transformation.<sup>35</sup> In several studies, the relative expression level of *CCNB2* was found to be significantly higher in patients with cancer than in normal controls and individuals with benign disease. Another study showed that overexpression of *CCNB2* protein was related to the clinical progression and poor prognosis in patients with NSCLC, suggesting that *CCNB2* may be a biomarker of NSCLC.<sup>36</sup> Finally, overexpression of *CCNB2* protein has been

shown to be related to clinical progression and poor prognosis in hepatocellular carcinoma and nasopharyngeal carcinoma.<sup>37,38</sup>

Cyclin A2, encoded by *CCNA2*, is another cyclin family member and cell cycle regulator. The protein binds to and activates cyclin-dependent kinase 2, thereby facilitating the  $G_1/S$  and  $G_2/M$  transitions.<sup>39</sup> *CCNA2* is also a prognostic biomarker for ER-positive breast cancer,<sup>40</sup> and overexpression of *CCNA2* in tumor tissue predicts poor survival in patients with pancreatic ductal adenocarcinoma.<sup>41</sup>

DNA topoisomerase II alpha, encoded by the *TOP2A* gene, modulates DNA topology during transcription by catalyzing the breakage and recombination of double-stranded and is also involved in DNA transcription and replication, chromatid separation, and chromosome condensation.<sup>42,43</sup> The *TOP2A* gene has been used as a target for several anticancer drugs; however, mutations in *TOP2A* are associated with acquired resistance. Moreover, decreased enzyme activity may be involved in ataxia-telangiectasia. In previous studies, *TOP2A* was shown to be a therapeutic target for adrenocortical carcinoma and neuroblastoma tumors,<sup>44,45</sup> and *TOP2A* gene amplification has been used to predict the response to anthracycline therapy in breast cancer.<sup>46</sup>

There were some limitations to our study. First, although we repeated our experiments independently three times, some

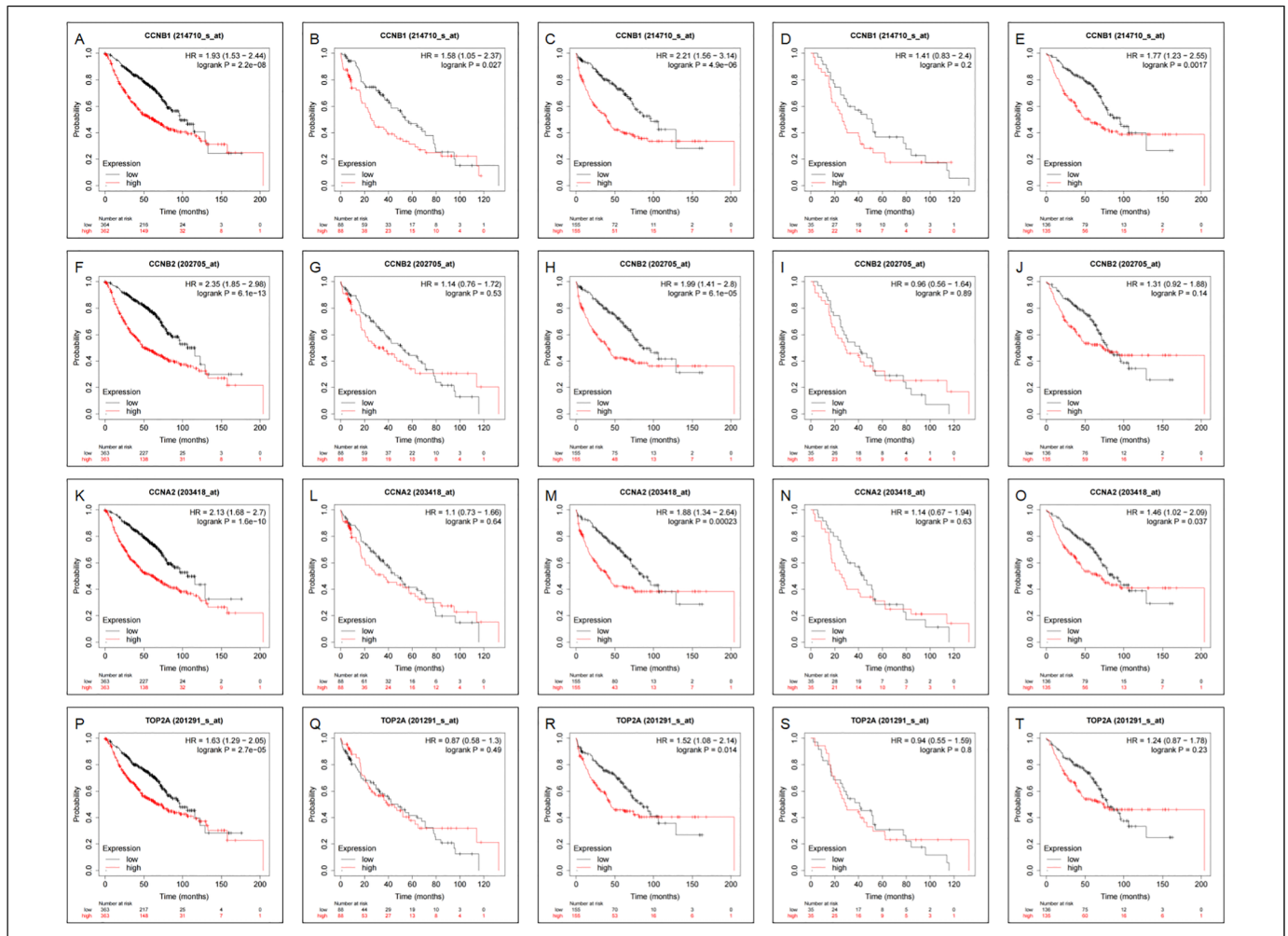


**Figure 9. Predictive ability of hub genes for overall survival in patients treated using different approaches.** Kaplan–Meier Plotter was used to evaluate overall survival rates according to high and low expression of (A–E) *CCNB1*, (F–J) *CCNB2*, (K–O) *CCNA2*, and (P–T) *TOP2A* in patients with NSCLC. (A, F, K, and P) Surgical margin-negative patients; (B, G, L, and Q) chemotherapy; (C, H, M, and R) no chemotherapy; (D, I, N, and S) radiotherapy; (E, J, O, and T) no radiotherapy.

target genes did not show significant differences, likely owing to the influence of random errors. Additionally, we only compared the expression levels of the target genes in one cancer cell line (A549 cells) and one normal lung cell line (HBE cells); therefore, the results should be interpreted with caution. In the future, additional experiments using more clinical specimens and different cell lines are required to verify our findings.

## Conclusion

In summary, in this study, we identified DEGs involved in the progression of NSCLC using integration of microarray data from multiple GEO datasets comprising large sample cohorts. We established a PPI network and determined the relationships of hub genes with diagnosis and prognosis in NSCLC. The diagnostic value and robustness of NSCLC

predicted by the hub genes were evaluated using the GEPIA web tool based on TCGA datasets. We finally verified the hub genes at the protein level using THPA. The upregulation of *CCNB1*, *CCNB2*, *CCNA2*, and *TOP2A* was verified in cell experiments. However, the functions of these hub genes in NSCLC must be verified in vitro and in vivo in future studies. In addition, we found that the predictive ability of the identified hub genes differed according to the treatment strategy used in the patients as well as the histological type of NSCLC. Overall, our findings provide important insights into the treatment of NSCLC based on genomics.

## Acknowledgments

The authors would like to thank Editage ([www.editage.com](http://www.editage.com)) for English language editing.

## Ethical Statement

Our study did not require an ethical board approval because it did not contain human or animal trials.

## Declaration of Conflicting Interests

The author(s) declared no potential conflicts of interest with respect to the research, authorship, and/or publication of this article.


## Funding

The author(s) disclosed receipt of the following financial support for the research, authorship, and/or publication of this article: This work was supported by the the Natural Science Foundation for Young Scientists of Hunan Province (grant number 2016JJ4099, 8150020951).

## Supplemental Material

Supplemental material for this article is available online.

## ORCID iD

Li Xie  <https://orcid.org/0000-0002-2634-6187>

## References

- Reck M, Heigener DF, Mok T, et al. Management of non-small-cell lung cancer: recent developments. *Lancet*. 2013;382:709-719.
- Allemani C, Weir HK, Carreira H, et al. Global surveillance of cancer survival 1995–2009: analysis of individual data for 25,676,887 patients from 279 population-based registries in 67 countries (CONCORD-2). *Lancet*. 2015;385:977-1010.
- Torre LA, Trabert B, DeSantis CE, et al. Ovarian cancer statistics, 2018. *CA Cancer J Clin*. 2018(68):284-296.
- Siegel RL, Miller KD, Jemal A. . Cancer statistics, 2018. *CA Cancer J Clin*. 2018;68:7-30.
- Ostheimer C, Evers C, Palm F, et al. Mortality after radiotherapy or surgery in the treatment of early stage non-small-cell lung cancer: a population-based study on recent developments. *J Cancer Res Clin Oncol*. 2019;145:2813-2822.
- Arbour KC, Riely GJ. Systemic therapy for locally advanced and metastatic non-small cell lung cancer: a review. *JAMA*. 2019;322:764-774.
- Prasad NB, Somervell H, Tufano RP, et al. Identification of genes differentially expressed in benign versus malignant thyroid tumors. *Clin Cancer Res*. 2008;14:3327-3337.
- Lusito E, Felice B, D'Ario G, et al. Unraveling the role of low-frequency mutated genes in breast cancer. *Bioinformatics*. 2019;35:36-46.
- Zhang L, Yang Y, Cheng L, et al. Identification of common genes refers to colorectal carcinogenesis with paired cancer and non-cancer samples. *Dis Markers*. 2018;2018:3452739.
- Sun M, Song H, Wang S, et al. Integrated analysis identifies microRNA-195 as a suppressor of hippo-YAP pathway in colorectal cancer. *J Hematol Oncol*. 2017;10:79.
- Li J, Wang W, Xia P, et al. Identification of a five-lncRNA signature for predicting the risk of tumor recurrence in patients with breast cancer. *Int J Cancer*. 2018;143:2150-2160.
- Hu X, Peng Q, Zhu J, et al. Identification of miR-210 and combination biomarkers as useful agents in early screening non-small cell lung cancer. *Gene*. 2020;729:144225.
- Wang K, Chen R, Feng Z, et al. Identification of differentially expressed genes in non-small cell lung cancer. *Aging*. 2019;11:11170-11185.
- Saigusa D, Motoike IN, Saito S, et al. Impacts of NRF2 activation in non-small-cell lung cancer cell lines on extracellular metabolites. *Cancer Sci*. 2020;111:667-678.
- Sanchez-Palencia A, Gomez-Morales M, Gomez-Capilla JA, et al. Gene expression profiling reveals novel biomarkers in non-small cell lung cancer. *Int J Cancer*. 2011;129:355-364.
- Kadara H, Fujimoto J, Yoo SY, et al. Transcriptomic architecture of the adjacent airway field cancerization in non-small cell lung cancer. *J Natl Cancer Inst*. 2014;106, dju004.
- Lu TP, Tsai MH, Lee JM, et al. Identification of a novel biomarker, SEMA5A, for non-small cell lung carcinoma in nonsmoking women. *Cancer Epidemiol Biomarkers Prev*. 2010;19:2590-2597.
- Barrett T, Wilhite SE, Ledoux P, et al. NCBI GEO: archive for functional genomics data sets—update. *Nucleic Acids Res*. 2013;41:D991-D995.
- Huang da W, Sherman BT, Lempicki RA. Systematic and integrative analysis of large gene lists using DAVID bioinformatics resources. *Nat Protoc*. 2009;4:44-57.
- Szklarczyk D, Franceschini A, Kuhn M, et al. The STRING database in 2011: functional interaction networks of proteins, globally integrated and scored. *Nucleic Acids Res*. 2011;39: D561-D568.
- Shannon P, Markiel A, Ozier O, et al. Cytoscape: a software environment for integrated models of biomolecular interaction networks. *Genome Res*. 2003;13:2498-2504.
- Gyorffy B, Lanczky A, Szallasi Z. Implementing an online tool for genome-wide validation of survival-associated biomarkers in ovarian-cancer using microarray data from 1287 patients. *Endocr Relat Cancer*. 2012;19:197-208.
- Tang Z, Li C, Kang B, et al. GEPIA: a web server for cancer and normal gene expression profiling and interactive analyses. *Nucleic Acids Res*. 2017;45:W98-W102.
- Lu L, Wu M, Lu Y, et al. MicroRNA-424 regulates cisplatin resistance of gastric cancer by targeting SMURF1 based on GEO database and primary validation in human gastric cancer tissues. *Onco Targets Ther*. 2019;12:7623-7636.
- Fu QF, Liu Y, Fan Y, et al. Alpha-enolase promotes cell glycolysis, growth, migration, and invasion in non-small cell lung cancer through FAK-mediated PI3 K/AKT pathway. *J Hematol Oncol*. 2015;8(22).
- Hou J, Aerts J, den Hamer B, et al. Gene expression-based classification of non-small cell lung carcinomas and survival prediction. *PLoS One*. 2010;5:e10312.
- Duma N, Santana-Davila R, Molina JR. Non-small cell lung cancer: epidemiology, screening, diagnosis, and treatment. *Mayo Clin Proc*. 2019;94:1623-1640.
- Hyun SY, Rosen EM, Jang YJ. Novel DNA damage checkpoint in mitosis: mitotic DNA damage induces re-replication without cell

- division in various cancer cells. *Biochem Biophys Res Commun.* 2012;423:593-599.
29. Wang X, Yu Q, Zhang Y, et al. Tectonic 1 accelerates gastric cancer cell proliferation and cell cycle progression in vitro. *Mol Med Rep.* 2015;12:5897-5902.
  30. Falero-Perez J, Sorenson CM, Sheibani N. Retinal astrocytes transcriptome reveals Cyp1b1 regulates the expression of genes involved in cell adhesion and migration. *PLoS One.* 2020;15:e0231752.
  31. Ding K, Li W, Zou Z, et al. CCNB1 Is a prognostic biomarker for ER + breast cancer. *Med Hypotheses.* 2014;83:359-364.
  32. El-Huneidi W, Shehab NG, Bajbouj K, et al. *Micromeria fruticosa* induces cell cycle arrest and apoptosis in breast and colorectal cancer cells. *Pharmaceuticals.* 2020;13.
  33. Liu A, Zeng S, Lu X, et al. Overexpression of G2 and S phase-expressed-1 contributes to cell proliferation, migration, and invasion via regulating p53/FoxM1/CCNB1 pathway and predicts poor prognosis in bladder cancer. *Int J Biol Macromol.* 2019;123:322-334.
  34. Arora S, Singh P, Rahmani AH, et al. Unravelling the role of miR-20b-5p, CCNB1, HMGA2 and E2F7 in development and progression of non-small cell lung cancer (NSCLC). *Biology (Basel).* 2020;9.
  35. Daldello EM, Luong XG, Yang CR, et al. Cyclin B2 is required for progression through meiosis in mouse oocytes. *Development.* 2019;146.
  36. Qian X, Song X, He Y, et al. CCNB2 Overexpression is a poor prognostic biomarker in Chinese NSCLC patients. *Biomed Pharmacother.* 2015;74:222-227.
  37. Li R, Jiang X, Zhang Y, et al. Cyclin B2 overexpression in human hepatocellular carcinoma is associated with poor prognosis. *Arch Med Res.* 2019;50:10-17.
  38. Qian D, Zheng W, Chen C, et al. Roles of CCNB2 and NKX3-1 in nasopharyngeal carcinoma. *Cancer Biother Radiopharm.* 2020;35:208-213.
  39. Li X, Ma XL, Tian FJ, et al. Downregulation of CCNA2 disturbs trophoblast migration, proliferation, and apoptosis during the pathogenesis of recurrent miscarriage. *Am J Reprod Immunol.* 2019;82:e13144.
  40. Zhou H, Lv Q, Guo Z. Transcriptomic signature predicts the distant relapse in patients with ER + breast cancer treated with tamoxifen for five years. *Mol Med Rep.* 2018;17:3152-3157.
  41. Dong S, Huang F, Zhang H, et al. Overexpression of BUB1B, CCNA2, CDC20, and CDK1 in tumor tissues predicts poor survival in pancreatic ductal adenocarcinoma. *Biosci Rep.* 2019;39.
  42. Liu T, Zhang H, Yi S, et al. Mutual regulation of MDM4 and TOP2A in cancer cell proliferation. *Mol Oncol.* 2019;13:1047-1058.
  43. Yu X, Davenport JW, Urtishak KA, et al. Genome-wide TOP2A DNA cleavage is biased toward translocated and highly transcribed loci. *Genome Res.* 2017;27:1238-1249.
  44. Gao Z, Man X, Li Z, et al. Expression profiles analysis identifies the values of carcinogenesis and the prognostic prediction of three genes in adrenocortical carcinoma. *Oncol Rep.* 2019;41:2440-2452.
  45. Hou JY, Baptiste C, Hombalegowda RB, et al. Vulvar and vaginal melanoma: a unique subclass of mucosal melanoma based on a comprehensive molecular analysis of 51 cases compared with 2253 cases of nongynecologic melanoma. *Cancer.* 2017;123:1333-1344.
  46. Eltohamy MI, Badawy OM, El kinaai N, et al. Topoisomerase II alpha gene alteration in triple negative breast cancer and its predictive role for anthracycline-based chemotherapy (Egyptian NCI patients). *Asian Pac J Cancer Prev.* 2018;19:3581-3589.